Isotopic evidence of nitrate degradation by a zero-valent iron permeable reactive barrier: Batch experiments and a field scale study

A. Grau-Martínez[1], C. Torrentó[1], R. Carrey[1], A. Soler[1], N. Otero[1,2]

[1]Grup MAiMA, Mineralogia Aplicada, Geoquímica i Geomicrobiologia, Departament de Mineralogia, Petrologia i Geologia Aplicada, SIMGEO UB-CSIC, Facultat de Ciències de la Terra, Universitat de Barcelona (UB), C/ Martí i Franquès, s/n, 08028 Barcelona, Spain.

[2]Serra Hunter Fellow, Generalitat de Catalunya, Spain.

Corresponding author: Clara Torrentó (clara.torrento@ub.edu)

Abstract

Permeable reactive barriers (PRBs) filled with zero-valent iron (ZVI) are a well-known remediation approach to treat groundwater plumes of chlorinated volatile organic compounds as well as other contaminants. In field implementations of ZVI-PRBs designed to treat these contaminants, nitrate consumption has been reported and has been attributed to direct abiotic nitrate reduction by ZVI or to denitrification by autochthonous microorganisms using the dissolved hydrogen produced from ZVI corrosion. Isotope tools have proven to be useful for monitoring the performance of nitrate remediation actions. In this study, we evaluate the use of isotope tools to assess the effect of ZVI-PRBs on the nitrate fate for the further optimization of full-scale applications. Laboratory batch experiments were performed using granular cast ZVI and synthetic nitrate solutions at pH 4-5.5 or nitrate-containing groundwater (pH=7.0) from a field site where a ZVI-PRB was installed. The experimental results revealed nitrate attenuation and ammonium production for both types of experiments. In the field site, the chemical and isotopic data demonstrated the occurrence of ZVI-induced abiotic nitrate reduction and denitrification in wells located close to the ZVI-PRB. The isotopic characterization of the laboratory experiments allowed us to monitor the efficiency of the ZVI-PRB at removing nitrate. The results show the limited effect of the barrier (nitrate reduction of

26   less than 15-20%), probably related to its non-optimal design. Isotope tools were therefore proven to

27   be useful tools for determining the efficacy of nitrate removal by ZVI-PRBs at the field scale.

28   **Keywords**: groundwater remediation, passive treatment system, abiotic nitrate reduction,

29   denitrification, multi-isotope analysis.

1. Introduction

31   Nitrate (NO_3^-) contamination in groundwater is a common and increasing global problem that affects

32   drinking water supplies around the world. Biological denitrification is the major nitrate removal

33   mechanism under natural conditions. However, in many contaminated aquifers, the activity of

34   nitrate-reducing bacteria is limited by the availability of electron donors (Rivett et al., 2008).

35   Therefore, over the last couple of decades, various remediation techniques have been explored for

36   groundwater clean-up (Khan et al., 2004). One of the innovative technologies used for in situ

37   remediation of contaminated groundwater is the use of permeable reactive barriers (PRBs) (USEPA,

38   2002; Tratnyek et al., 2003). This in situ remediation technique involves the interception of

39   groundwater flow to remove contaminants by physical, chemical or biological processes. Several

40   constructed PRBs filled with zero-valent iron (ZVI) have been used to treat groundwater

41   contaminated with chlorinated volatile organic compounds (O'Hannesin and Gillham, 1998; Phillips

42   et al., 2010; Wilkin et al., 2014; Audí-Miró et al., 2015), chromium (VI) (Flury et al., 2009; Wilkin et al.,

43   2014), sulfates (Da-Silva et al., 2007), pesticides (Yang et al., 2010), explosives (Da-Silva et al., 2007;

44   Johnson and Tratnyek, 2008) or radionuclides, such as uranium (Gu et al., 2002a; Morrison et al.,

45   2002).

46   The success of these barriers has stimulated significant interest in the application of ZVI to other

47   contaminants, such as nitrate. Gu et al. (2002a) observed decreases in nitrate concentrations in

48   downgradient (and some upgradient) monitoring wells of a ZVI-PRB installed to remove the

49   radionuclides uranium and technetium. The decrease in the nitrate content was attributed to direct

50   abiotic nitrate reduction by ZVI or to denitrification by microorganisms that use the dissolved

51   hydrogen produced from ZVI corrosion. Morrison et al. (2002) also observed decreases in nitrate

contents in monitoring wells located in and around a ZVI-PRB installed in a former uranium milling

site for the removal of uranium and vanadium. Nitrate removal has also been reported in a ZVI pilot-

scale funnel-and-gate system designed to treat groundwater contaminated with trichloroethylene

(Yabusaki et al., 2001). Finally, Hosseini et al. (2018) demonstrated the efficiency in nitrate removal

from groundwater of non-pumping reactive wells (NPRWs) filled with a mixture of nano/micro ZVI in

bench-scale laboratory tests.

At the laboratory scale, numerous studies have demonstrated the effectiveness of ZVI for the abiotic

reduction of nitrate (Huang et al., 1998; Westerhoff and James, 2003; Huang and Zhang, 2004; Shin

and Cha, 2008, Liu et al., 2013; Zhang et al., 2017). The following reaction pathway (Eq. 1) has been

proposed to be the dominant one during abiotic nitrate reduction by ZVI (Yang and Lee, 2005;

Rodríguez-Maroto et al., 2009):

$$4Fe \tag{1}$$

Ammonium is the main product in nitrate reduction by ZVI (Huang et al., 1998; Li et al., 2010; Suzuki

et al., 2012), although other products, such as nitrite and nitrogen gas, have also been reported

(Choe et al., 2000; Shin and Cha, 2008). The main limitation in the application of ZVI-PRB to reduce

nitrate is therefore the generation of ammonium ions that are potentially toxic to aquatic organisms

at high concentrations (Shin and Chan, 2008; Hwang et al., 2011; Suzuki et al., 2012). Furthermore,

since nitrate is corrosive to ZVI, clogging processes may affect the performance of hydraulic PRBs (Gu

et al., 2002a; Ritter et al., 2002), especially at high nitrate concentrations (Kamolpornwijit et al.,

2003; Liang et al., 2005).

The combined use of ZVI and a carbon substrate for in situ biochemical denitrification has been

considered in recent years and has been shown to be effective at the laboratory scale in improving

denitrification rates (Della Rocca et al., 2006; Della Rocca et al., 2007). Huang et al. (2015) and

Hosseini and Tosco (2015) demonstrated the efficacy of nitrate removal from contaminated

groundwater by a combination of ZVI and carbon substrates (pine bark, beech sawdust and maize

77   cobs) in laboratory tests. Liu et al. (2013) demonstrated that the main role of ZVI in two-layer

78   permeable reactive barriers consisting of ZVI and activated carbon immobilizing denitrifying

79   microbial consortia was as an oxygen capturing reagent and not for direct nitrate reduction.

80   When iron metal is immersed in water under anaerobic conditions, its corrosion produces cathodic

81   hydrogen following Eq. 2 (Reardon, 1995). This cathodic hydrogen can be used as an electron donor

82   by autotrophic denitrifiers for nitrate reduction (Till et al., 1998) (Eq. 3).

83   (2)

84   (3)

85   The use of this cathodic hydrogen as an energy source to support bacterial growth has been

86   demonstrated for several types of anaerobic pure cultures, including autotrophic denitrifiers (Till et

87   al., 1998) and methanogenic, homoaceotogenic, and sulfate-reducing bacteria (Daniels et al., 1987;

88   Rajagopal and LeGall, 1989). An indigenous hydrogenotrophic consortium is thus likely to eventually

89   develop around a hydrogen-producing ZVI-PRB. Gu et al. (2002b) found that the depletion of

90   dissolved oxygen and the production of cathodic hydrogen by ZVI corrosion in a ZVI-PRB designed for

91   the sequestration or removal of uranium provided a reducing environment favorable to many

92   hydrogen-consuming anaerobic microorganisms, such as sulfate and metal-reducing bacteria,

93   methanogens, and denitrifying bacteria. Da Silva et al. (2007) also identified several bacteria that

94   could utilize hydrogen produced during anaerobic ZVI corrosion in groundwater samples from within

95   and around a ZVI-PRB installed for the remediation of a site contaminated with explosives.

96   Denitrifying bacteria may therefore greatly increase the rate and extent of nitrate reduction in the

97   reducing zone of a ZVI-PRB. The combination of ZVI-driven nitrate reduction with denitrification by

98   autohydrogenotrophic denitrifying bacteria has been proved at the laboratory scale, resulting in an

99   increase in the nitrate removal rate and a decrease in ammonium release (Dejournett and Alvarez,

100   2000; Shin and Cha, 2008; An et al., 2009).

101 Induced nitrate attenuation at the field scale may be masked by several processes, such as

102 dispersion, diffusion or dilution (mixing), which can change the nitrate concentration in groundwater.

103 The isotopic fractionation of N (ε^{15}N) and O (ε^{18}O) of dissolved nitrate calculated following a Rayleigh

104 distillation process in lab-scale experiments of denitrification with ZVI may be used in future studies

105 to assess the behavior of the system in the field and optimize full-scale applications. To the authors'

106 knowledge, the oxygen and nitrogen isotopic fractionations associated with nitrate reduction by ZVI

107 have not yet been reported in the literature. The potential use of the in situ measurement of the

108 isotopic composition of nitrate to assess the effectiveness of ZVI-PRBs at removing nitrate has yet to

109 be evaluated.

110 The main objective of this study is therefore to determine the nitrogen and oxygen isotope

111 fractionations (ε^{15}N and ε^{18}O) associated with the ZVI-driven nitrate reduction reaction to investigate

112 the potential of isotope analyses to assess the fate of nitrate in a PRB-ZVI installed in a site

113 contaminated with volatile organic compounds where high nitrate concentrations in groundwater

114 are detected.

115 **2. Study area**

116 The study site is located in the industrial area of Granollers, 20 km NW of Barcelona, Catalonia. An

117 automotive industry that used tetrachloroethene and trichloroethene as degreasers operated in the

118 area from 1965 to 1989. Groundwater contamination by chlorinated solvents resulted from the

119 discharge of industrial waters into a seepage pit located to the south of the plant (close to MW17

120 well, Fig. 1). The lithology of the site is mainly composed of an alternation of sand and silt Miocene

121 sediments in a clay matrix that extends from 4 m to a minimum of 14 m in depth (Audí-Miró et al.,

122 2015). Above these materials, there are 4 m of quaternary glacis formed by the Miocene materials

123 that are mainly composed of poorly structured clays and silts. The water table of the aquifer is

124 located at an average depth of 5.4 ± 2.1 m. The deepest water table (approximately 8 m) was

125 measured at the base and at the top of the studied valley area (length of the studied area is 900 m).

126 At approximately 300 m from the top of this area, the water table was located closer to the surface

127 (approximately 3 m in depth) (Fig. 1). The average water table variation due to seasonal changes was

128 -0.5 ± 0.9 m. The groundwater flow direction was NE to W-SW, and the flow velocity was estimated

129 at approximately 0.16 m day^{-1} at the shallow quaternary clay depth and 0.84 m day^{-1} at the sandier

130 Miocene depth (Audí-Miró et al., 2015). The site is crossed by the Can Ninou Creek along which a

131 piezometer network was installed (Fig. 1).

132 In 2009, contaminated soil from the source area was removed, and in 2010, a ZVI-PRB was installed

133 (Audí-Miró et al., 2015). The ZVI-PRB was built approximately 320 m downgradient of the

134 contaminated source, transverse to the creek, from NW to SE (Fig. 1). The top of the PRB was placed

135 4-5 m below the ground surface, and its size is 20 m long, 5 m high and 60 cm thick, with a 3% (v/v)

136 granular cast ZVI inside a sand matrix.

137 The piezometer network consists of 12 conventional wells and 5 multilevel wells. The conventional

138 wells were installed between 2005 and 2010 along the east bank of the creek (expected direction of

139 groundwater flow) from the source area to 900 m downgradient of the creek (Fig. 1). The wells

140 consists of 50 mm inner diameter PVC pipes screened from 3 to 12 m depth, except MW17 and

141 OMW5 wells, screened from 5 to 10 m and from 7 to 11 m, respectively. In March 2012, five

142 additional wells were installed surrounding the barrier, two immediately upgradient of the PRB and

143 three immediately downgradient. These five wells have a multilevel sampling system installed

144 consisting of a bundle of small-diameter (5 mm outer diameter) PTFE tubes surrounding the

145 monitoring well casing and positioned at different depths, providing the possibility to obtain several

146 depth discrete groundwater samples from the same borehole (from 2 to 13.5 m depth, with a 0.5 m

147 interval).

148 **3. Materials and Methods**

149 **3.1 Laboratory-scale experiments**

150 Batch experiments were carried out in triplicate using 40 mL glass bottles. Each bottle contained 6.75

151 g of cast iron (92% purity, Gotthart Maier Metall pulver GmbH, Rheinfelden, Germany) and 35 mL of

152   a nitrate-containing aqueous solution. Prior to the experiment, the ZVI was acid-cleaned with 1 N

153   degassed HCl for 1 h and then rinsed five times with degassed deionized water (Milli-Q Plus UV,

154   Millipore™, Billerica, Massachusetts, USA), dried and stored inside a sterilized and anaerobic

155   chamber with a N_2 atmosphere at +28 ± 2 °C (Matheson and Tratnyek, 1994; Dayan et al., 1999;

156   Slater et al., 2002). In the chamber, UV light was used to sterilize the iron. The ZVI was weighed

157   before and after the treatment to verify that it was dry. The specific surface area of the cast iron

158   determined by N_2 gas adsorption (BET method) (Brunauer et al., 1938) was $1.624 \pm 0.007 \ m^2 \ g^{-1}$. The

159   size of the iron particles ranged between 0.4 to 2.0 mm, with an average diameter of 1.2 mm

160   (Torrentó et al., 2017).

161   Three different solutions were used: Milli-Q water (pH=5.5) (MQ experiments), a pH 4 HCl 0.1 M

162   solution (pH4 experiments) and groundwater (pH=7.0) from a piezometer (PZ10) located

163   immediately upgradient of the ZVI-PRB installed in the study site (PRB experiments). All of the

164   synthetic solutions contained 1.93 mM of nitrate, whereas the content of nitrate in the groundwater

165   sample was 2.93 mM.

166   The experiments were set up inside the glove box with an argon atmosphere to avoid the presence

167   of O_2. After preparation, the bottles were immediately covered with aluminum foil to avoid oxidation

168   due to light, and they were removed from the glove box and rotated on a horizontal roller table

169   (Wheaton, Millville, New Jersey, USA) at 60 rpm about their longitudinal axes. Experimental runs

170   lasted for 8 days, and aqueous samples were taken daily using sterile syringes purged with N_2. All of

171   the samples were filtered through a 0.2 μm Millipore® filter and preserved at 4 °C in darkness prior

172   to further analysis. The concentrations of nitrogen species and the $\delta^{15}N$ and $\delta^{18}O$ of dissolved nitrate

173   were measured in selected samples.

174   **3.2 Sampling surveys**

175   To assess the effect of the ZVI-PRB on the nitrate fate, three sampling campaigns were performed in

176   June 2012, October 2012 and March 2013. Both the conventional and multilevel wells were sampled

177   (Fig. 1). The conventional wells were sampled using a portable pump, whereas for the multilevel

178 wells, disposable 60 mL polypropylene sterile syringes were used to raise the water from each small-

179 diameter PTFE tube. In order to obtain depth discrete samples, the water volume sampled from each

180 tube was minimized as much as possible to prevent interference with the adjacent tubes. For each

181 sampling campaign, selected depths were sampled. For both conventional and multilevel wells, the

182 wells were purged before sampling.

183 The groundwater piezometric level was measured and the physicochemical parameters (pH,

184 temperature, dissolved oxygen and conductivity) were measured on site using a flow-through cell

185 (Eijkelkamp, Netherlands) connected in line with the sampling tubes to avoid contact with the

186 atmosphere. A Multi3410 multi-parameter meter (WTW, Weilheim, Germany) was used. Samples

187 were collected and preserved in plastic bottles that were filled completely to avoid the oxidation of

188 species from contact with the atmosphere. Samples were preserved at 4 °C and passed through a 0.2

189 μm filter in darkness prior to further analysis. In most of the collected samples, the nitrate, nitrite

190 (NO_2^-), ammonium (NH_4^+) and cation concentrations were measured. The $\delta^{15}N$ and $\delta^{18}O$ of dissolved

191 nitrate were measured in selected samples collected in March 2013. The δ^2H_{H2O} and $\delta^{18}O_{H2O}$ of water

192 were analyzed in a subset of samples.

193 **3.3 Analytical methods**

194 Nitrate and nitrite concentrations were determined by high performance liquid chromatography

195 (HPLC) with a WATERS 515 HPLC pump, IC-PAC anion columns and a WATERS 432 detector.

196 Ammonium was analyzed using ionic chromatography (DIONEX ICS5000). For the analysis of major

197 cations, samples were acidified with 1% nitric acid. The cation concentrations were determined by

198 inductively coupled plasma-optical emission spectrometry (ICP-OES, Perkin-Elmer Optima 3200 RL).

199 Chemical analyses were conducted at the "Centres Científics i Tecnològics" of the Universitat de

200 Barcelona (CCiT-UB) and "Institut Català de Recerca de l'Aigua (ICRA)".

201 The $\delta^{15}N$ and $\delta^{18}O$ of dissolved nitrate were determined using a modified cadmium reduction

202 method (McIlvin and Altabet, 2005; Ryabenko et al., 2009). Briefly, nitrate was converted to nitrite

203 through spongy cadmium reduction and then to nitrous oxide using sodium azide in an acetic acid

204 buffer. Simultaneous $\delta^{15}N$ and $\delta^{18}O$ analyses of the produced N_2O were carried out using a Pre-Con

205 (Thermo Scientific) coupled to a Finnigan MAT-253 Isotope Ratio Mass Spectrometer (IRMS, Thermo

206 Scientific). δ^2H_{H2O} was measured by pyrolysis using a Thermo-Quest high-temperature conversion

207 analyzer (TC/EA) unit with a Finnigan MAT Delta C IRMS. $\delta^{18}O_{H2O}$ was measured using the CO_2

208 equilibrium technique following the standard method (Epstein and Mayeda, 1953) using a GasBench

209 coupled to the MAT-253 IRMS. The notation was expressed in terms of δ relative to international

210 standards (V-SMOW for δ^2H_{H2O} and $\delta^{18}O_{H2O}$ and V-AIR for $\delta^{15}N$). According to Coplen (2011), several

211 international and laboratory standards were interspersed among the sequences for the

212 normalization of analyses. The analytical reproducibility by repeated analysis of both international

213 and internal reference samples of known isotopic composition was ± 1‰ for $\delta^{15}N_{NO3}$, ± 1.5‰ for

214 $\delta^{18}O_{NO3}$, ± 1‰ for δ^2H_{H2O}, and ± 0.3‰ for $\delta^{18}O_{H2O}$. Samples for isotopic analyses were prepared at the

215 MAiMA laboratory and determined at CCiT-UB.

216 **3.4 Isotope fractionation calculation**

217 Isotopic fractionation during nitrate transformation is commonly calculated in laboratory

218 experiments in which the conditions are well constrained, no other sinks affect the nitrate pool and

219 the changes in the concentration and the isotopic composition of nitrate can be considered to be

220 exclusively determined by the nitrate transformation process. The process is modeled following a

221 Rayleigh distillation. Using the Rayleigh equation (Eq. 4), the isotopic fractionation factor α can be

222 obtained (Aravena and Robertson, 1998; Mariotti et al., 1988):

223   (4)

224 where C_0 and C_t are the nitrate concentrations at the beginning and at a given time (t), respectively

225 (mmol L^{-1}), and R_0 and R_t denote the ratios of heavy versus light isotopes at the beginning and at time

226 t, respectively, which are calculated according to Eq. 5.

227   (5)

228   where δ is the isotopic composition of ^{15}N and ^{18}O (‰). The term (α - 1) is calculated from the slope

229   of the regression analysis in double-logarithmic plots, [ln(R_t/R_0)] over [ln(C_t/C_0)], according to Eq. 4

230   and is converted to isotopic fractionation (ε^{15}N and ε^{18}O) following Eq. 6.

231   (6)

232   With the ε values obtained in the laboratory experiments, the percentage of denitrification at the

233   field scale can be calculated according to Eq. 7 using either εN or εO, or both.

234   ————   —————   (7)

235   The isotope signature of the original nitrate ($\delta_{initial}$) is usually assumed to correspond to that of the

236   determined nitrate source or to the lowest value found in the field site.

237   **4. Results and discussion**

238   **4.1 Batch experiments: chemical data**

239   Complete removal of nitrate was observed within 7 days in all batch experiments (Supplementary

240   Material, Table S1). In all experiments, ammonium was produced (maximum values of 2.47 mM for

241   PRB, 1.47 mM for MQ and 1.40 mM for pH4), whereas no significant nitrite contents (maximum

242   values for all experiments ranged from 0.01 mM to 0.03 mM, achieved during the first 2-3 days) were

243   detected (Table S1). The nitrogen mass balance in the experiments shows that ammonium and nitrite

244   account for approximately 50-100% of the nitrate removal in the PRB and 45-75% in the MQ and pH4

245   experiments (Table S1). According to Chen et al. (2005), sorption of ammonium onto mineral oxides

246   produced by ZVI corrosion (Westerhoff and James, 2003) was ruled out. Thus, gaseous N species

247   should account for closing the nitrogen mass balance. Production of N_2 (g) has been proposed to be a

248   by-product of ZVI-driven nitrate reduction by other authors (Yang and Lee, 2005) in similar

249   experiments. Furthermore, abiotic homogeneous or heterogeneous reduction of nitrite coupled to

250   the oxidation of the Fe(II) released from the ZVI may also occur, which is also a source of N_2O

251   (Buchwald et al., 2016).

252   Previous studies (Cheng et al., 1997; Choe et al., 2000; Su and Puls, 2004) have suggested that ZVI-

253   driven nitrate reduction is first order with respect both nitrate concentration and ZVI concentration.

254   Excluding the effect of ZVI concentration, the reaction was thus assumed to be of pseudo first order

255   with respect to nitrate concentration. Data for nitrate concentration versus time were fit to a

256   pseudo-first-order rate model:

257   $$\qquad\qquad\qquad\qquad\qquad\qquad — \qquad\qquad\qquad\qquad\qquad\qquad\qquad\qquad (8)$$

258   where C is the nitrate concentration, t is time and k' is the pseudo-first-order rate constant. The k'

259   was obtained using the integrated form of this equation, from the slope of the regression lines of the

260   ln C/C_0 vs. time graph (Fig. 2), where C_0 is the initial nitrate concentration. Uncertainty was obtained

261   from the 95% confidence intervals. The nitrate consumption rate in the experiments with

262   groundwater (PRB experiments) was faster (k'=0.86 ± 0.09 d^{-1}) than that in the experiments with

263   synthetic solutions (MQ and pH4 experiments, k'=0.46 ± 0.04 d^{-1} for both experiments), suggesting

264   additional nitrate degradation by autochthonous bacteria. The higher nitrate removal in biotic batch

265   experiment (PRB) may be attributed to denitrification by autochthonous denitrifiers, which use the

266   hydrogen or Fe(II) generated by ZVI corrosion as electron donors (Till et al., 1998; Shin and Cha,

267   2008; An et al., 2009; Jamieson et al., 2018; Xu et al., 2018; Zhang et al., 2019).

268   The surface-area-normalized reaction rate constants (k_{SA}) were calculated for comparison with other

269   studies following Eq. 9 (Johnson et al., 1996):

270   $$\qquad\qquad\qquad\qquad\qquad\qquad\qquad\qquad\qquad\qquad\qquad\qquad\qquad\qquad\qquad\qquad (9)$$

271   where a_S is the ZVI specific surface area ($m^2\,g^{-1}$) and ρm is the mass concentration of ZVI (g L^{-1}).

272   The obtained k' values correspond to k_{SA} values of 2.8 ± 0.3×10^{-3} L m^{-2} d^{-1} for the PRB experiment and

273   1.6 ± 0.1×10^{-3} L m^{-2} d^{-1} for both the MQ and pH4 experiments. For the latter experiments, the

274   obtained k_{SA} values are within the range reported for chemical nitrate reduction by ZVI (1.1×10^{-4} to

275 7.2 L m^{-2} d^{-1} for pH between 7 and 9.5, and 2.4×10^{-3} to 12.3 L m^{-2} d^{-1} for pH values of 3-6.5, Alowitz

276 and Scherer, 2002; Su and Puls, 2004; Choe et al., 2004; Ginner et al., 2004; Miehr et al., 2004).

277 Both abiotic batch experiments (pH4 and MQ) showed the same reaction rate, suggesting that at the

278 tested conditions (pH=4 for the pH4 experiment, pH=5.5 for the MQ experiment, respectively), ZVI-

279 driven nitrate reduction was independent of the pH. Nevertheless, at pH values relevant to ZVI-PRBs

280 (pH from 6.5 to 9), slower rates have generally been observed at higher pH values (Hu et al., 2001;

281 Alowitz and Scherer, 2002; Miehr et al., 2004; Westerhoff and James, 2003; Ginner et al., 2004).

282 In the case of the experiment with combined abiotic nitrate reduction and denitrification (PRB

283 experiment, since the ZVI surface area is not reported in most previous studies, a comparison is

284 performed in terms of the pseudo-first-order rate constants. The k' value of the PRB experiment

285 (k'=0.86 ± 0.09 d^{-1}) is similar to that reported by Shin and Cha (2008) using a culture obtained from

286 activated sludge and anaerobic digester samples from a wastewater treatment plant (k'=0.97 d^{-1}),

287 even when the latter used nano ZVI. Previous studies using cast (Ginner et al., 2004) and nano (An et

288 al., 2009) ZVI in combination with pure cultures of denitrifying bacteria resulted in faster nitrate

289 removal rates (k' from 1.5 to 2.4 d^{-1}).

290 **4.2 Batch experiments: isotopic results**

291 All of the experiments showed considerable enrichment in both ^{15}N and ^{18}O in the remaining nitrate

292 over the course of the experiments (Table S1), confirming nitrate degradation. In the PRB

293 experiment, δ^{15}N increased from +8.2‰ to +154.9‰, whereas δ^{18}O increased from +5.4‰ to

294 +83.5‰. Similarly, the δ^{15}N-NO$_3^-$ in the MQ and pH4 experiments increased from +15.6‰ and

295 +15.9‰ to +133.2‰ and +135.9‰, respectively. The δ^{18}O values increased from +26.5‰ and

296 +29.3‰ to +78.2‰ and +79.9‰ in the MQ and pH4 experiments, respectively. The ϵ^{15}N and ϵ^{18}O

297 values in the experiments were obtained from the slope of the linear correlation between the

298 natural logarithm of the remaining fraction of the substrate, ln(C$_{residual}$/C$_{initial}$), where C refers to the

299 analyte concentration, and the determined isotope ratios, ln(R$_{residual}$/R$_{initial}$), following Eq. 4 (Fig. 3).

300 Uncertainty was obtained from the 95% confidence intervals. Obtained values are shown in Table 1.

301   The nitrogen isotopic fractionation (ε^{15}N) was -29.5 ± 2.7‰ for the PRB experiment, -37.7 ± 7.2‰ for

302   the MQ experiment and -36.1 ± 7.1‰ for pH4 experiment. The oxygen isotopic fractionation (ε^{18}O)

303   was -16.4 ± 1.1‰ for the PRB experiment, -17.2 ± 4.2‰ for the MQ experiment, and -16.1 ± 3.1‰

304   for the pH4 experiment (Fig. 3).

305   The isotope fractionation for abiotic nitrate reduction has not been reported to date; the obtained

306   values were thus compared with those reported for biotic denitrification. The ε^{15}N and ε^{18}O values

307   obtained in the present study fell within the range of the values reported in the literature for

308   denitrification in laboratory experiments (Grau-Martínez et al., 2017, and references therein). The

309   ε^{15}N values were similar to the values obtained by Barford et al. (1999) and Toyoda et al. (2005) for

310   heterotrophic denitrification by pure cultures. With regards to ε^{18}O, the obtained values were similar

311   to those reported by Wunderlich et al. (2012) for heterotrophic denitrification by pure cultures.

312   In all of the experiments, δ^{15}N showed a linear relationship with δ^{18}O, with slopes between 0.43 and

313   0.54, yielding ε^{18}O/ε^{15}N ratios of 0.54 ± 0.07 for the PRB experiment and 0.45 ± 0.02 and 0.43 ± 0.03

314   for the MQ and pH4 experiments, respectively (Fig. 4 and Table 1). A comparison of the obtained

315   slopes for the regression lines (ε^{18}O/ε^{15}N) was performed by analysis of covariance (ANCOVA).

316   Statistical significance was accepted at the $p<0.05$ level. Since they were highly consistent, the data

317   from the pH4 and MQ experiments were combined (Table 1). There is a significant statistical

318   difference between the slope obtained for the experiments with purely abiotic solutions (ε^{18}O/ε^{15}N=

319   0.43 ± 0.02) and that for the PRB experiment (ε^{18}O/ε^{15}N= 0.54 ± 0.07) (ANCOVA, $p=0.0003$). This

320   result leads to the potential application of this approach to distinguish ZVI-driven nitrate reduction

321   and additional degradation of nitrate by the action of autochthonous denitrifying bacteria in field

322   sites where ZVI-PRBs are installed.

323   **4.2.1 Insights from the ε^{18}O/ε^{15}N ratio during abiotic ZVI-driven nitrate reduction**

324   Abiotic nitrate reduction is the only process that acts in the MQ and pH4 batches. To the authors'

325   knowledge, no isotopic fractionation ratio (ε^{18}O/ε^{15}N) for abiotic nitrate reduction using ZVI has been

326   published to date. The ε^{18}O/ε^{15}N reported for heterogeneous and homogeneous chemical nitrite

327 reduction in the presence of dissolved Fe^{2+} showed higher values ($\varepsilon^{18}O/\varepsilon^{15}N$ from 0.7 to 1.7,

328 Buchwald et al., 2016; Grabb et al., 2017). Lower ratios can be produced by the incorporation of

329 oxygen isotopes from water into nitrite and the subsequent re-oxidation of nitrite to nitrate

330 (Wunderlich et al., 2013). Consequently, the isotopic equilibrium tends to reduce the $\varepsilon^{18}O$ values,

331 decreasing the $\varepsilon^{18}O/\varepsilon^{15}N$ ratio to values of 0.5. In this study, nitrite re-oxidation can be ruled out for

332 all of the experiments since the batch experiments were performed under anaerobic conditions and

333 nitrite accumulation was below 0.02 mM. Furthermore, in the pH4 and MQ experiments, with no

334 biotic competition, the dissolved Fe^{2+} released from ZVI favored fast chemical nitrite reduction over

335 any potential nitrate re-oxidation. In addition, the fast nitrate consumption and the high isotopic

336 composition of $\delta^{18}O_{NO3}$ observed (up to +83.5‰) allowed us to consider the equilibrium isotopic

337 fractionation between water and nitrate to be negligible compared with the kinetic isotopic

338 fractionation during nitrate reduction. Lower $\varepsilon^{18}O/\varepsilon^{15}N$ ratios have also been reported to be

339 produced by different enzymes involved in nitrate reduction (Granger et al., 2008). In this sense, the

340 activity of the periplasmic nitrate reductase (Nap) results in a $\varepsilon^{18}O/\varepsilon^{15}N$ value of ~0.6, whereas the

341 membrane-bound respiratory nitrate reductase (Nar) tends to produce a fractionation ratio of ~1.0

342 (Granger et al., 2008). The transformation of nitrate to ammonium by dissimilatory nitrate reduction

343 to ammonium (DNRA) is considered to mostly be catalyzed by this Nap complex (Kraft et al., 2011).

344 Therefore, the results of the MQ and pH4 experiments, without enzymatic function, suggest some

345 mechanistic control in the isotope fractionation ratios obtained for purely chemical nitrate reduction

346 by ZVI. On the other hand, although further research is needed, these results suggest that the use of

347 $\varepsilon^{18}O/\varepsilon^{15}N$ to distinguish between biotic (DNRA) and abiotic (ZVI-driven) production of ammonium

348 from nitrate reduction is limited.

349 **4.2.2 Insights from the $\varepsilon^{18}O/\varepsilon^{15}N$ ratio during combined abiotic ZVI-driven nitrate reduction and**

350 **denitrification**

351 In the PRB experiment, a biotic nitrate-reduction process was assumed to occur in combination with

352 a purely abiotic ZVI-driven nitrate reduction. This biotic nitrate reduction is likely to be autotrophic

353 denitrification by autochthonous denitrifying bacteria using the hydrogen or the Fe^{2+} released from

354 ZVI, although heterotrophic denitrification with the organic carbon present in groundwater or with

355 the biogenic acetate produced by homoacetogens that utilize cathodic hydrogen cannot be ruled out

356 (Zhang et al., 2019). From the kinetic data collected from all of the experiments (Fig. 2), the

357 proportion of the ZVI-driven nitrate reduction (pathway 1) in the overall degradation process

358 (pathway 1 + pathway 2) was calculated as the rate ratio of the two competing pathways (F =

359 $k'_1/(k'_1+ k'_2)$), showing a 52% contribution of purely abiotic ZVI-driven nitrate reduction.

360 The isotopic fractionation values ($\epsilon^{15}N$ and $\epsilon^{18}O$) for the denitrification process in the PRB

361 experiments (pathway 2) were then estimated using a Rayleigh-type equation for multiple competing

362 degradation pathways following first-order kinetics (Van Breukelen, 2007), as follows (Eq. 10):

363 $$\underline{\quad\quad}$$ (10)

364 where ϵ_1 is the isotope fractionation of pathway 1 (ZVI-driven nitrate reduction, i.e., experiments

365 pH4 and MQ), and ϵ_A is the isotope fractionation of the overall degradation process (i.e., the PRB

366 experiment). The obtained values of $\epsilon^{15}N$ (-15.5 ‰) and $\epsilon^{18}O$ (-20.5 ‰) for the denitrification

367 process in the PRB experiments were used to estimate the corresponding $\epsilon^{18}O/\epsilon^{15}N$ ratio ($\epsilon^{18}O/\epsilon^{15}N$

368 = 0.76) (Table 1).

369 During (heterotrophic and autotrophic) denitrification, the $\epsilon^{18}O/\epsilon^{15}N$ ratio reported in laboratory

370 studies ranged from 0.3 (Knöller et al., 2011) to 1.3 (Grau-Martínez et al., 2018) in freshwater

371 environments, whereas in marine environments, the fractionation ratio showed values of ~1.0

372 (Casciotti et al., 2002; Granger et al., 2004; Sigman et al., 2005). Autotrophic denitrification

373 experiments using pyrite (FeS_2) as an electron donor have shown a fractionation ratio of 0.87

374 (Torrentó et al., 2010). A $\epsilon^{18}O/\epsilon^{15}N$ ratio of 0.9 has been reported for autotrophic denitrification with

375 aqueous Fe^{2+} in groundwater (Smith et al., 2017). To the authors' knowledge, the isotopic

376 fractionation ratio for hydrogenotrophic denitrification has not been reported and cannot be

377 compared with the obtained results. Factors such as the pH, salinity or carbon sources showed no

378 effect on the $\varepsilon^{18}O/\varepsilon^{15}N$ ratio (Granger et al., 2008; Wunderlich et al., 2012). Nevertheless, the

379 microbial community composition can impact the ratio at which the nitrogen and oxygen of nitrate

380 are processed during denitrification (Dähnke and Thamdrup, 2016). Overall, despite the fact that the

381 differences between the $\varepsilon^{18}O/\varepsilon^{15}N$ ratios obtained for PRB and those of the pH4 and MQ

382 experiments suggest the occurrence of denitrification in the former, the responsible reaction could

383 not be addressed.

384 **4.3 Field study**

385 **4.3.1 Hydrochemical characterization**

386 The results of the chemical characterization of the field samples are detailed in the Supplementary

387 Material (Table S2). The pH values analyzed upgradient of the barrier ranged between 6.7 and 9.0,

388 whereas the pH values of the multilevel (BR1, BR2, BR3, BR4, BR5) and conventional (PZ10 and PZ11)

389 wells located close to the barrier ranged between 4.4 and 7.5, except for higher values that were

390 found in a few points in June 2012. The PZ4 well, located at the west end of the barrier, presented

391 pH values of approximately 7 in June 2012 and approximately 9 in March 2013. Finally, the pH values

392 in conventional wells downgradient of the ZVI-PRB ranged from 5.4 to 8.8, similar to the values

393 observed upgradient of the PRB. The pH analyzed downgradient of the barrier therefore does not

394 correspond to the common increase of pH that usually occurs after the corrosion of iron with water

395 (Eq. 2), probably due to the relatively high pH-buffering capacity of the aquifer.

396 The chemical data indicated that reducing conditions prevailed in the aquifer: dissolved oxygen (DO)

397 was found in most of the points below 2 mg L^{-1}; dissolved manganese was present at a concentration

398 up to 1.39 mg L^{-1}; and dissolved iron was detected at a concentration up to 2.5 mg L^{-1}. Furthermore,

399 Audí-Miró et al. (2015) demonstrated that these conditions were conducive to the biodegradation of

400 chlorinated ethenes by reductive dechlorination.

401 To assess the effect of ZVI-PRB on nitrogen compounds, the evolution of the nitrate, nitrite and

402 ammonium concentrations was monitored along the flow path, upgradient and downgradient of the

403 ZVI-PRB. The samples in the focus area (MW-17) showed negligible nitrate concentrations

404 throughout the sampling period, indicating that reducing conditions prevailed. In this well, the

405 presence of dissolved manganese and iron was up to 1.3 mg L^{-1} and 2.5 mg L^{-1}, respectively,

406 confirming reducing conditions. Downgradient of the focus area, wells OMW5, PZ1, PZ2 and PZ3

407 showed low nitrate values (up to 29.4 mg L^{-1}, Table S2) in all campaigns.

408 Figure 5 shows the evolution of the nitrate concentrations in the wells closer to the barrier (the

409 conventional wells PZ10, PZ4 and PZ11 and the multilevel wells BR1, BR2, BR3, BR4 and BR5) for the

410 three sampling surveys. Overall, there are no significant differences in the nitrate concentration with

411 depth. The nitrate concentrations in these wells increase throughout the sampling period, with

412 median concentrations of approximately 79 mg L^{-1} (June 2012), 141 mg L^{-1} (October 2012) and 177

413 mg L^{-1} (March 2013).

414 Regarding multilevel wells located immediately upgradient and downgradient of the PRB, the nitrate

415 concentrations are always higher in piezometers BR1 and BR3, both of which are located to the NW

416 of the barrier, and lower in piezometers BR2, BR4 and BR5, which are located to the SE of the PRB.

417 These results are probably due to the lateral input of water with a high nitrate concentration (the

418 conventional well PZ4, located to the NW of the barrier, has the highest nitrate concentration).

419 Because of this observed lateral input, the percentage of nitrate attenuation due to the barrier was

420 calculated from the nitrate contents by comparing BR1 to BR3 and BR2 to BR4 and BR5. Comparing

421 BR1 to BR3, a slight decrease in the nitrate concentration was observed in June 2012 and October

422 2012 (16% decrease) and March 2013 (11% decrease). Comparing BR2 to BR4 and BR5, a higher

423 decrease in the nitrate concentration was observed in June 2012 (26 to 72%) and October 2012

424 (30%), whereas in March 2013, contradictory percentages were obtained (an increase of 10%

425 between BR2 and BR4 and an 18% decrease between BR2 and BR5). Therefore, the observed

426 changes in the nitrate concentration from immediately upgradient to downgradient of the PRB

427 suggest the occurrence of nitrate degradation processes related to the ZVI-PRB, although isotope

428 data are required to confirm this hypothesis. No significant differences in nitrite concentrations were

429 observed upgradient and downgradient of the barrier, since in most cases, they were below the

430 detection limit (0.01 mg L^{-1}). The ammonium concentration slightly increased from BR2 to BR4 and

431 BR5 in June 2012, but values were always below 0.4 mg L^{-1}. No significant ammonium was detected

432 downgradient of the barrier, indicating that if nitrate was transformed to ammonium through a

433 reaction with the ZVI, it was oxidized again to nitrate or absorbed into soil materials.

434 The wells located far downgradient of the ZVI-PRB (PZ7, PZ8 and PZ9) showed nitrate concentrations

435 ranging from 14 mg L^{-1} to 80 mg L^{-1} (Table S2). For the three sampling campaigns, lower values were

436 observed in PZ7 and increased downgradient. This downgradient increase could reflect the

437 contribution of lateral inputs or the fact that the barrier was bypassed. In these points, no significant

438 differences in nitrite and ammonium concentrations were observed.

4.3.2 Evidence of nitrate reduction: insights from isotope data

440 The results of the isotopic characterization of the field samples are detailed in the Supplementary

441 Material (Table S3). The samples from the focus zone (MW17) could not be analyzed because the

442 nitrate concentrations were below the detection limit, which is in agreement with the observed

443 reducing conditions and the natural biodegradation of chlorinated solvents described previously by

444 Audí-Miró et al. (2015). Wells OMW5 and PZ2, located upgradient of the PRB, showed isotopic

445 values of approximately +15‰ for $\delta^{15}N_{NO3}$ and +11‰ for $\delta^{18}O_{NO3}$. These high values suggest that

446 natural attenuation of nitrate takes place upgradient of the ZVI-PRB. Audí-Miró et al. (2015) also

447 observed the natural attenuation for chlorinated solvents in these wells.

448 Figure 6 shows the $\delta^{15}N_{NO3}$ and $\delta^{18}O_{NO3}$ from the survey of March 2013 at the multilevel wells (BR 1

449 to 5) and the conventional wells located closer to the PRB (PZ4 and PZ10). The isotopic values of the

450 main potential nitrate sources are represented as well: nitrate fertilizers, ammonium fertilizers, soil

451 nitrate and animal manure or sewage (Vitòria et al., 2004; Kendall et al., 2007; Xue et al., 2009). The

452 range of $\delta^{18}O$ of nitrate derived from nitrification of ammonium fertilizers, soil nitrogen and/or

453 manure/sewage (from +1.9‰ to +3.1‰) was estimated according to Anderson and Hooper (1983)

454 using the range of $\delta^{18}O_{H2O}$ measured in groundwater samples (between -7.6‰ and -5.1‰). All of the

18

samples presented isotope ratios compatible with those for soil organic nitrogen and manure/sewage, with variable degree of denitrification. The nitrogen and oxygen isotope values of the samples located immediately upgradient of the PRB ranged from +6.2 to +13.9‰ for $\delta^{15}N$ and from +4.9 to +9.7‰ for $\delta^{18}O$, whereas the values of the samples located immediately downgradient of the PRB ranged from +13.2 to +18.1‰ for $\delta^{15}N$ and from +9.0 to +12.6‰ for $\delta^{18}O$, except for BR5-11, where low isotope ratios were obtained (+9.6‰ and +6.8‰, respectively). Taking into account that the PRB is located at a depth of approximately 10 m, a bypass effect probably occurs at the BR5-11 point, where low isotope ratios were obtained. It is important to note that PZ4 and BR1 showed higher values of $\delta^{15}N_{NO3}$ and $\delta^{18}O_{NO3}$ than those for BR2, which confirms that both PZ4 and BR1 are affected by a lateral input of groundwater with higher nitrate concentration and different isotope signature. Therefore, in general, higher isotopic values were detected immediately downgradient than immediately upgradient of the PRB, confirming the existence of nitrate attenuation processes. Furthermore, the samples showed a positive correlation (r^2=0.89) between $\delta^{15}N_{NO3}$ and $\delta^{18}O_{NO3}$ and were aligned following a $\epsilon^{18}O/\epsilon^{15}N$ ratio of 0.63 (Fig. 6), which is consistent with denitrification (Kendall et al., 2007) and with the values obtained in the PRB experiments.

We thus assumed the occurrence of combined ZVI-driven nitrate reduction and denitrification. To quantify the efficiency of the ZVI-PRB in removing nitrate, Eq. 7 was applied using the $\epsilon^{15}N$ and $\epsilon^{18}O$ values calculated in the PRB batch experiments ($\epsilon^{15}N$ = -29.5±2.7‰ and $\epsilon^{18}O$ = -16.4±1.1‰). Since some wells were affected with the lateral input of groundwater contaminated with nitrate with a different isotope signature, two $\delta_{initial}$ values were used: (1) the initial isotopic composition of the PRB experiment (+8.2‰ for $\delta^{15}N_{NO3}$ and +5.4‰ for $\delta^{18}O_{NO3}$), which corresponds to water extracted from PZ10, located upgradient of the barrier but not affected by the lateral input of PZ4 (model % DEN), and (2) the average isotope ratios of the PZ4 and BR1 wells (+12.8‰ for $\delta^{15}N_{NO3}$ and +8.5‰ for $\delta^{18}O_{NO3}$), which are clearly affected by the lateral input of PZ4 (model % DEN Lateral). Figure 8 shows the ranges of percentage of nitrate degradation obtained applying the two models and the isotope signature of the multilevel wells and the PZ4 and PZ10 wells. The %DEN Lateral model was thus used

481 for the well BR3, which was clearly affected by the lateral input. The degree of nitrate attenuation in

482 the samples of this well ranged between 10 and 20%. Similar though slightly lower percentages (5 to

483 15%) were obtained for samples of the BR5 well, for which the %DEN model was used. Finally, the

484 results from samples from BR4 suggest that this well might also be affected by the lateral input of

485 PZ4, and thus the %DEN Lateral model was used, obtaining a degree of degradation of approximately

486 15%.

487 Overall, the nitrate removal percentages calculated using the isotopic model are in agreement with

488 those calculated using the nitrate concentration. On well BR5, this percentage was slightly

489 overestimated using only chemical data, because bypass could only be detected using isotopic data.

490 The isotopic data also allowed the identification of the influence of the lateral input of PZ4 not only

491 on BR3 but also on BR4. Therefore, stable isotopes of dissolved nitrate are powerful tools to assess

492 the efficacy of the barrier for nitrate removal.

493 For further quantitative evaluation of the effect of the ZVI-PRB on the nitrate fate, by means of the

494 data obtained in the laboratory experiments, the contribution of the purely abiotic ZVI-driven

495 reaction in overall nitrate consumption was calculated using the equation proposed by Van

496 Breukelen (2007) for estimating the distribution (F) of two competing pathways based on the two-

497 dimensional isotopes approach (Eq. 11):

498 $$\overline{\rule{3cm}{0pt}}$$ (11)

499 where $\varepsilon^{18}O_A/\varepsilon^{15}N_A$ corresponds to the ratio of 0.63 obtained for the wells located immediately

500 upgradient and downgradient of the PRB (Fig. 6). The $\varepsilon^{18}O$ and $\varepsilon^{15}N$ values obtained in the laboratory

501 experiments were used for pathway 1 (purely abiotic ZVI-PRB driven nitrate reduction, i.e., MQ

502 experiment, Table 1) and pathway 2 (denitrification, i.e., values obtained by Eq. 10, Table 1). The

503 results show that approximately 30% of the nitrate consumption was related to the purely abiotic

504 nitrate reduction by the ZVI included in the PRB.

505 Overall, the isotopic results confirm that nitrate reduction is taking place in the barrier, though it has

506 a limited effect (maximum attenuation degree of 15-20%). This result is in agreement with the

507 previous results of Audí-Miró et al. (2015), in which the effectiveness of the ZVI-PRB to reduce

508 chlorinated solvents was tested using isotopic tools and was demonstrated to be even less efficient

509 than for nitrate (maximum of 10%). The O-N slope of field values fit the expected slope obtained in

510 the laboratory experiments well, indicating that isotopes are an excellent tool to determine the

511 efficacy of the ZVI-PRB at the field scale.

512 **5. Conclusions**

513 In laboratory experiments with sterilized ZVI and synthetic nitrate solutions, ZVI induced nitrate

514 reduction, mainly releasing ammonium to solution (after 7 days, ammonium accounted for 70-80%

515 of nitrate reduction). For assessing the fate of nitrate in the contaminated site of Granollers, where a

516 ZVI-PRB was installed, batch experiments were also performed using ZVI and groundwater from the

517 study area. In these experiments, the main final product was also ammonium (80-100%). The faster

518 nitrate removal rates of the latter suggest denitrification processes in addition to the ZVI-driven

519 purely abiotic nitrate reduction. Isotopic fractionation associated to ZVI-induced nitrate attenuation

520 processes was determined for the first time. The significant statistical difference between the

521 isotope $\varepsilon^{18}O/\varepsilon^{15}N$ ratios obtained for the experiments with purely abiotic solutions (0.43±0.02) and

522 for the PRB experiment (0.54±0.07) shows the potential for the use of this approach to distinguish

523 ZVI-driven nitrate reduction and additional degradation of nitrate by the action of autochthonous

524 bacteria in field sites where ZVI-PRBs are installed. Data obtained from the laboratory experiments

525 were used for assessing the fate of nitrate in the study area. Combining chemical and isotope data, it

526 was demonstrated that the ZVI-PRB installed in the study area locally induced nitrate attenuation,

527 though the barrier had a limited effect (less than 15-20%). As Audí-Miró et al. (2015) noted for

528 chlorinated solvents, this low efficiency in nitrate removal was probably related to the non-optimal

529 design of the PRB, including a ZVI amount (3%) that was too low and an insufficient length of the

530 PRB, which was responsible for the bypass occurrence. Further evaluation of the fate of ammonium

21

531 downgradient of the ZVI-PRB is required since no ammonium was detected in groundwater.

532 Laboratory experiments can be performed to assess the potential retention of the generated

533 ammonium by the aquifer materials through ion exchange and/or adsorption. Further work is

534 required to identify the reaction responsible for the additional nitrate removal in experiments with

535 ZVI and groundwater from the field site and to study the denitrifying microbial community developed

536 around the ZVI-PRB. Overall, this study highlights the potential of isotope tools for determining the

537 efficacy of nitrate removal by ZVI-PRBs at the field scale. This information might be crucial for

538 mitigating existing pollution in water resources and improving remediation actions.

539

546 **References**

547 Alowitz, M.J., Scherer, M.M. (2002). Kinetics of nitrate, nitrite, and Cr(VI) reduction by iron metal.
548 Environm. Sci. Technol. 36, 299-306.

549 An, Y., Li, T.L., Jin, Z.H., Dong, M.Y., Li, Q.Q. (2009). Decreasing ammonium generation using
550 hydrogenotrophic bacteria in the process of nitrate reduction by nanoscale zero-valent iron. Sci.
551 Total Environ. 407, 5465-5470.

552 Anderson, K.K., Hooper, A.B., (1983). O_2 and H_2O are each the source of O in NO_2 produced from NH_3
553 by Nitrosomas: ^{15}N-NMR evidence. FEBS Lett. 64, 236-240.

554 Aravena, R., Robertson, W.D. (1998). Use of multiple isotope tracers to evaluate denitrification in
555 ground water: Study of nitrate from a large-flux septic system plume. Ground Water 36, 975-982.

556 Audí-Miró, C., Cretnik, S., Torrentó, C., Rosell, M., Shouakar-Stash, O., Otero, N., Palau, J., Elsner, M.,
557 Soler, A. (2015). C, Cl and H compound specific isotope analysis to assess natural versus Fe(0) barrier-
558 induced degradation of chlorinated ethenes at a contaminated site. J. Hazar. Mater. 299, 747-754.

559 Brunauer, S., Emmet, P. H., Teller, E. (1938). Adsorption of gases on multimolecular layers. J. Am.
560 Chem. Soc. 60, 309-319.

561 Buchwald, C., Grabb, K., Hansel, C.M., Wankel, S.D. (2016). Constraining the role of iron in
562 environmental nitrogen transformations: dual stable isotope systematics of abiotic NO_2^- reduction by
563 Fe(II) and its production of N_2O. Geochim. Cosmochim. Ac. 186, 1-12.

564 Casciotti, K.L., Sigman, D.M., Hastings, M.G., Böhlke, J.K., Hilkert, A. (2002). Measurement of the
565 oxygen isotopic composition of nitrate in seawater and freshwater using the denitrifier method.
566 Anal. Chem. 74, 4905-4912.

567 Chen, Y.M., Li, C.W., Chen, S.S. (2005). Fluidized zero valent iron bed reactor for nitrate removal.
568 Chemosphere 59, 753-759.

569 Cheng, I.F., Muftikian, R., Fernando, Q., Korten, N. (1997). Reduction of nitrate to ammonia by zero-
570 valent iron. Chemosphere 35, 2689-2695.

571 Choe, S., Chang, Y.Y., Hwang, K.Y., Khim, J. (2000). Kinetics of reductive denitrification by nanoscale
572 zero-valent iron. Chemosphere 41, 1307-1311.

573 Choe, S., Liljestrand, H.M., Khim, J. (2004). Nitrate reduction by zero-valent iron under different pH
574 regimes. Appl. Geochem. 19, 335-342.

575 Coplen, T.B. (2011). Guidelines and recommended terms for expression of stable-isotope-ratio and
576 gas-ratio measurement results. Rapid Commun. Mass Sp. 25, 2538-2560.

577 Dähnke, K., Thamdrup, B. (2016). Isotope fractionation and isotope decoupling during anammox and
578 denitrification in marine sediments. Limnol. Oceanogr. 61, 610-624.

579 Daniels, L., Belay, N., Rajagopal, P., Weimer, J. (1987). Bacterial methanogenesis and the growth of
580 CO_2 with elemental iron as the sole source of electrons. Science 237, 509-511.

581 Da Silva, M.L.B., Johnson, R.L., Alvarez, P.J.J. (2007). Microbial characterization of groundwater
582 undergoing treatment with a permeable reactive iron barrier. Environ. Eng. Sci. 24, 1122-1127.

583   Dayan, H., Abrajano, T., Sturchio, N.C., Winsor, L. (1999). Carbon isotopic fractionation during

584   reductive dehalogenation of chlorinated ethenes by metallic iron. Org. Geochem. 30, 755-763.

585   Della Rocca, C., Belgiorno, V., Meric, S. (2006). An heterotrophic/autotrophic denitrification (HAD)

586   approach for nitrate removal from drinking water. Process. Biochem. 41, 1022-1028.

587   Della Rocca, C., Belgiorno, V., Meric, S. (2007). Overview of in-situ applicable nitrate removal

588   processes. Desalination 204, 46-62.

589   Dejournett, T.D., Alvarez, P.J. (2000). Combined microbial-Fe (0) treatment system to remove nitrate

590   from contaminated groundwater. Biorem. J. 4, 149-154.

591   Epstein, S., Mayeda, T. (1953). Variation of O^{18} content of waters from natural sources. Geochim.

592   Cosmochim. Ac. 4, 213-224.

593   Flury, B., Eggenberger, U., Mäder, U. (2009). First results of operating and monitoring an innovative

594   design of a permeable reactive barrier for the remediation of chromate contaminated groundwater.

595   Appl. Geochem. 24, 687-696.

596   Ginner, J.L., Alvarez, P.J., Smith, S.L., Scherer, M.M. (2004). Nitrate and nitrite reduction by Fe0:

597   influence of mass transport, temperature, and denitrifying microbes. Environm. Eng. Sci. 21, 219-229.

598   Grabb, K. C., Buchwald, C., Hansel, C.M., Wankel, S.D. (2017). A dual nitrite isotopic investigation of

599   chemodenitrification by mineral-associated Fe (II) and its production of nitrous oxide. Geochim.

600   Cosmochim. Ac., 196, 388-402.

601   Granger, J., Sigman, D.M., Needoba, J.A., Harrison, P.J. (2004). Coupled nitrogen and oxygen isotope

602   fractionation of nitrate during assimilation by cultures of marine phytoplankton. Limnol. Oceanogr.

603   49, 1763-1773

604   Granger, J., Sigman, D.M., Lehmann, M.F., Tortell, P.D. (2008). Nitrogen and oxygen isotope

605   fractionation during dissimilatory nitrate reduction by denitrifying bacteria. Limnol. Oceanogr. 53,

606   2533-2545.

607   Grau-Martínez, A., Torrentó, C., Carrey, R., Rodríguez-Escales, P., Domènech, C., Ghiglieri, G., Soler,

608   A., Otero, N. (2017). Feasibility of two low-cost organic substrates for inducing denitrification in

609   artificial recharge ponds: Batch and flow-through experiments. J. Contam. Hydrol. 198, 48-58.

610   Grau-Martínez, A., Folch, A., Torrentó, C., Valhondo, C., Barba, C., Domènech, C., Soler, A., Otero, N.
611   (2018). Monitoring induced denitrification during managed aquifer recharge in an infiltration pond. J.
612   Hydrol. 561, 123-135.

613   Gu, B., Watson, D.B., Phillips, D.H., Liang, L. (2002a). Biogeochemical, mineralogical, and hydrological
614   characteristics of an iron reactive barrier used for treatment of uranium and nitrate, In: D.L. Naftz, S.
615   J. Morrison, J.A. Davis, C.C. Fuller (Eds.), Groundwater remediation of trace metals, radionuclides,
616   and nutrients with Permeable Reactive Barriers. Academic Press, New York, pp. 305-342.

617   Gu, B., Watson, D.B., Wu, L., Phillips, D.H., White, C., Zhou, J.Z. (2002b). Microbiological
618   characteristics in a zero-valent iron reactive barrier. Environ. Monit. Assess. 77, 293-309.

619   Hosseini, S.M., Altaie-Ashtiani, B., Kholghi, M. (2011). Bench-scaled nano-FeO permeable reactive
620   barrier for nitrate removal. Ground Water Monit. R. 31 (4), 82-94

621   Hosseini, S.M., Tosco, T. (2015). Integrating NZVI and carbon substrates in a non-pumping reactive
622   wells array for the remediation of a nitrate contaminated aquifer. J. Contam. Hydrol. 179, 182-195.

623   Hosseini, S.M., Tosco, T., Ataie-Ashtiani, B., Simmons, C.T. (2018). Non-pumping reactive wells filled
624   with mixing nano and micro zero-valent iron for nitrate removal from groundwater: Vertical,
625   horizontal, and slanted wells. J. Contam. Hydrol. 210, 50-64.

626   Hu, H.-Y., Naohiro, G., Koichi, F. (2001) Effect of pH on the reduction of nitrite in water by metallic
627   iron. Water Res. 35, 2789-2793.

628   Huang, Y.H., Zhang, T.C. (2004). Effects of low pH on nitrate reduction by iron powder. Water Res. 38,
629   2631-2642.

630   Huang, C.P., Wang, H.W., Chiu, P.C. (1998). Nitrate reduction by iron at near neutral pH. J. Environ.
631   Engineer. ASCE 128, 604-611.

632   Huang, G., Huang, Y., Hu, H., Liu, F., Zhang, Y., Deng, R. (2015). Remediation of nitrate-nitrogen
633   contaminated groundwater using a pilot-scale two-layer heterotrophic-autotrophic denitrification
634   permeable reactive barrier with spongy iron/pine bark. Chemosphere 130, 8-16.

635   Hwang, Y.H., Kim, D., Shin, H. (2011). Mechanism study of nitrate reduction by nano zero valent iron.
636   J. Hazard. Mater. 185, 1513-1521.

637 Jamieson, J., Prommer, H., Kaksonen, A.H., Sun, J., Siade, A. J., Yusov, A., Bostick, B. (2018).
638 Identifying and quantifying the intermediate processes during nitrate-dependent iron (II) oxidation.
639 Environm. Sci. Technol. 52, 5771-5781.

640 Johnson, T.L., Scherer, M.M., Tratnyek, P.G. (1996) Kinetics of halogenated organic compound
641 reduction by iron metal. Environ. Sci. Technol. 30, 2634-2640.

642 Johnson, R., Tratnyek, P. (2008). Remediation of Explosives in Groundwater Using a Zero-Valent Iron
643 Permeable Reactive Barrier. ESTCP Project ER-0223, Oregon Health and Science University, Portland.

644 Kamolpornwijit, W., Liang, L., West, O.R., Moline, G.R., Sullivan, A.B. (2003). Preferential flow path
645 development and its influence on long-term PRB performance: column study. J. Contam. Hydrol. 66,
646 161-178.

647 Kendall, C., Elliott, E.M., Wankel, S.D. (2007). Tracing anthropogenic inputs of nitrogen to
648 ecosystems. In: Michener, R.H., Lajtha, K. (Eds.), Stable isotopes in Ecology and Environmental
649 Science. Blackwell Publishing, pp. 375-449.

650 Khan, F.I., Husain, T., Hejazi, R. (2004). An overview and analysis of site remediation technologies. J.
651 Envirn. Manage. 71, 95-122.

652 Knöller, K., Vogt, C., Haupt, M., Feisthauer, S., Richnow, H.H. (2011). Experimental investigation of
653 nitrogen and oxygen isotope fractionation in nitrate and nitrite during denitrification.
654 Biogeochemistry 103, 371-384.

655 Kraft, B., Strous, M., Tegetmeyer, H.E. (2011). Microbial nitrate respiration – genes, enzymes and
656 environmental distribution. J. Biotechnol. 155, 104-117.

657 Liang, L., Moline, G.R., Kamolpornwijit, W., West, O.R. (2005). Influence of hydrogeochemical
658 processes on zero-valent iron reactive barrier performance: A field investigation. J. Contam. Hydrol.
659 78, 291-312.

660 Liu, Y.S., Ying, G.G., Shareef, A., Kookana, R.S. (2013). Biodegradation of three selected
661 benzotriazoles in aquifer materials under aerobic and anaerobic conditions. J. Contam. Hydrol. 151,
662 131-139.

663 Mariotti, A., Landreau, A., Simon, B. (1988). [15]N isotope biogeochemistry and natural denitrification
664 process in groundwater application to the chalk aquifer of northern France. Geochim. Cosmochim.
665 Ac. 52, 1869-1878.

666   Matheson, L.J., Tratnyek, P.G. (1994). Reductive dehalogenation of chlorinated methanes by iron
667   metal. Environ. Sci. Technol. 28, 2045-2053.

668   McIlvin, M.R., Altabet, M.A. (2005). Chemical conversion of nitrate and nitrite to nitrous oxide for
669   nitrogen and oxygen isotopic analysis in freshwater and seawater. Anal. Chem. 77, 5589-5595.

670   Miehr, R., Tratnyek, P.G., Bandstra, J.Z., Scherer, M.M., Alowitz, M.J., Bylaska, E.J. (2004). Diversity of
671   contaminant reduction reactions by zerovalent iron: Role of the reductate. Environm. Sci. Technol.
672   38, 139-147.

673   Morrison, S. J.; Carpenter, C. E.; Metzler, D. R.; Bartlett, T. R.; Morris, S. A. (2002). Desing and
674   performance of a Permeable Reactive Barrier for containment of uranium, arsenic, selenium,
675   vanadium, molybdenum and nitrate at Monticello, Utah. In: Naftz, D.L., Morrison, S.J., Fuller, C.C.,
676   Davis, J.A. (Eds.) Handbook of groundwater remediation using Permeable Reactive Barriers.
677   Applications to radionuclides, trace Metals, and nutrients. Academic Press, New York, pp. 371-399.

678   O'Hannesin, S.F., Gillham, R.W. (1998). Long-term performance of an in situ "iron wall" for
679   remediation of VOCs. Ground Water 36, 164-170.

680   Phillips, D.H. (2010). Permeable reactive barriers: a sustainable technology for cleaning contaminated
681   groundwater in developing countries. Desalination 251, 352-359.

682   Rajagopal, B., LeGall, J. (1989). Utilization of cathodic hydrogen by hydrogen oxidizing bacteria. Appl.
683   Microbiol. Biotechnol. 31, 406-412.

684   Reardon, E.J. (1995). Anaerobic corrosion of granular iron: measurement and interpretation of
685   hydrogen evolution rates. Environ. Sci. Technol. 29, 2936-294

686   Ritter, K., Odziemskowski, M.S., Gillham, R.W. (2002). An in situ study of the role of surface films on
687   granular iron in the permeable iron wall technology. J. Contam. Hydrol. 55, 87-111.

688   Rivett, M.O., Buss, S.R., Morgan, P., Smith, J.W.N., Bemment, C.D. (2008). Nitrate attenuation in
689   groundwater: a review of biogeochemical controlling processes. Water Res. 42, 4214-4232.

690   Rodríguez-Maroto, J.M., García-Herruzo, F., García-Rubio, A., Gómez-Lahoz, C., Vereda-Alonso, C.
691   (2009). Kinetics of the chemical reduction of nitrate by zero-valent iron. Chemosphere 74, 804-809.

692   Ryabenko, E., Altabet, M.A., Wallace, D.W.R. (2009). Effect of chloride on the chemical conversion of
693   nitrate to nitrous oxide for δ^{15}N analysis. Limnol. Oceanogr. 7, 545-552.

694   Shin, K., Cha, D.K. (2008). Microbial reduction of nitrate in the presence of nanoscale zero-valent
695   iron. Chemosphere, 72, 257-262.

696   Sigman, D.M., Granger, J., DiFiore, P.J., Lehmann, M.M., Ho, R., Cane, G., van Geen, A. (2005).
697   Coupled nitrogen and oxygen isotope measurements of nitrate along the eastern North Pacific
698   margin. Global Biogeochem. Cy. 19.

699   Slater, G.F., Lollar, B.S., King, A., O'Hannesin, S. (2002). Isotopic fractionation during reductive
700   dechlorination of trichloroethene by zero-valent iron: influence of surface treatment. Chemosphere
701   49, 587-596.

702   Smith, R.L., Kent, D.B., Repert, D.A., Böhlke, J.K. (2017). Anoxic nitrate reduction coupled with iron
703   oxidation and attenuation of dissolved arsenic and phosphate in a sand and gravel aquifer. Geochim.
704   Cosmochim. Ac. 196, 102-120.

705   Su, C., Puls, R.W. (2004). Significance of iron (II, III) hydroxycarbonate green rust in arsenic
706   remediation using zero valent iron in laboratory column test. Environ. Sci. Technol. 38, 5224-5231.

707   Suzuki, T., Moribe, M., Oyama, Y., Niinaem M. (2012). Mechanism of nitrate reduction by zero-valent
708   iron: Equilibrium and kinetics studies. Chem. Engineer. J. 183, 271-277.

709   Till, B.A., Weathers, J.L., Alvarez, J.J.P. (1998). Fe(0)-Supported autotrophic denitrification. Environ.
710   Sci. Technol. 32, 634-639.

711   Torrentó, C., Cama, J., Urmeneta, J., Otero, N., Soler, A. (2010). Denitrification of groundwater with
712   pyrite and *Thiobacillus denitrificans*. Chemical Geology, 278, 80-91.

713   Torrentó, C., Palau, J., Rodríguez-Fernández, D., Heckel, B., Meyer, A., Domènech, C., Rosell, M.,
714   Soler, A., Elsner, M., Hunkeler, D. (2017). Carbon and chlorine isotope fractionation patterns
715   associated with different engineered chloroform transformation reactions. Environ. Sci. Technol. 51,
716   6174-6184

717   Toyoda, S., Mutobe, H., Yamagishi, H., Yoshida, N., Tanji, Y. (2005). Fractionation of N_2O isotopomers
718   during production by denitrifier. Soil Biol. Biochem. 37, 1535-1545.

719   Tratnyek, P.G., Scherer, M.M., Johnson, T.L., Matheson, L.J. (2003). Permeable reactive barriers of
720   iron and other zero-valent metals. In: Tarr, M.A. (Ed.) Chemical degradation methods for wastes and
721   pollutants: Environmental and industrial applications. CRC Press, p.p. 371-422.

722 U.S. EPA (2002). Field Applications of In Situ Remediation Technologies: Permeable Reactive Barriers.
723 U.S. Environmental Protection Agency, Office of Solid Waste and Emergency Response, Washington,
724 DC.

725 Van Breukelen, B.M. (2007). Extending the Rayleigh equation to allow competing isotope
726 fractionating pathways to improve quantification of biodegradation. Environ. Sci. Technol. 41, 4004-
727 4010.

728 Vitòria, L., Otero, N., Canals, A., Soler, A. (2004). Fertilizer characterization: isotopic data (N, S, O, C
729 and Sr). Environ. Sci. Technol. 38, 3254-3262.

730 Westerhoff, P., James, J. (2003). Nitrate removal in zero-valent iron packed columns. Water Res. 37,
731 1818-1830.

732 Wilkin, R.T., Acree, S.D., Ross, R.R., Puls, R.W., Lee, T.R., Woods, L.L. (2014). Fifteen-year assessment
733 of a permeable reactive barrier for treatment of chromate and trichloroethylene in groundwater. Sci.
734 Total Environ. 468-469, 186-194.

735 Wunderlich, A., Meckenstock, R., Einsiedl, F. (2012). Effect of different carbon substrates on nitrate
736 stable isotope fractionation during microbial denitrification. Environ. Sci. Technol. 46, 4861-4868.

737 Wunderlich, A., Meckenstock, R.U., Einsiedl, F. (2013). A mixture of nitrite-oxidizing and denitrifying
738 microorganisms affects the $\delta^{18}O$ of dissolved nitrate during anaerobic microbial denitrification
739 depending on the $\delta^{18}O$ of ambient water. Geochim. Cosmochim. Ac. 119, 31-45.

740 Xu, C., Wang, X., An, Y., Yue, J., Zhang, R. (2018). Potential electron donor for nanoiron supported
741 hydrogenotrophic denitrification: H_2 gas, Fe0, ferrous oxides, Fe^{2+} (aq), or Fe^{2+} (ad)?. Chemosphere,
742 202, 644-650.

743 Xue, D., Botte, J., De Baets, B., Accoe, F., Nestler, A., Taylor, P., Van Cleemput, O., Berglund, M.,
744 Boeckkx, P. (2009). Present limitations and future prospects of stable isotopes methods for nitrate
745 source identification in surface and groundwater. Water Res. 43, 1159-1170.

746 Yabusaki, S., Cantrell, K., Sass, B., Steefel, C. (2001). Multicomponent reactive transport in an in situ
747 zero-valent iron cell. Environm. Sci. Technol. 35, 1493-1503.

748 Yang, S.-C., Lei, M., Chen, T.-B., Li, X.-Y., Liang, Q., Ma, C. (2010). Application of zerovalent iron (Fe(0))
749 to enhance degradation of HCHs and DDX in soil from a former organochlorine pesticides
750 manufacturing plant. Chemosphere 79, 727-732.

751   Yang, G.C.C., Lee, H.L. (2005). Chemical reduction of nitrate by nanosized iron: kinetics and pathways.

752   Water Res. 39, 884-894.

753   Zhang, Y., Douglas, G.B., Pu, L., Zhao, Q., Tang, Y., Xu, W., Luo, B., Hong, W., Cui, L., Ye, Z. (2017).

754   Zero-valent iron-facilitated reduction of nitrate: Chemical kinetics and reaction pathways. Sci. Total

755   Environm. 598, 1140-1150.

756   Zhang, Y., Douglas, G. B., Kaksonen, A. H., Cui, L., Ye, Z. (2019). Microbial reduction of nitrate in the

757   presence of zero-valent iron. Sci. Total Environm. 646, 1195-1203.

1   **Figure captions**

2   **Figure 1.** Map of the study site. The location of the wells installed along Can Ninou Creek,

3   the location of the ZVI-PRB, and the distribution of the multilevel wells around the ZVI-PRB,

4   as well as the piezometric surfaces and groundwater flow lines, are represented. Cross

5   section along the creek from the source area to 1000 m downstream. The lithology and the

6   screened interval of each well is exposed, as well as the water table indicated by the

7   blue triangles. Modified from Audi-Miró et al. (2015).

8   **Figure 2**. Evolution of ln (C/C$_0$) for both nitrate and ammonium over time in all of the batch

9   experiments. The linear regression lines and high correlation values (R^2) evidenced pseudo-

10   first-order kinetics.

11   **Figure 3**. δ^{18}O (A) and δ^{15}N (B) of nitrate against the natural logarithm of the nitrate

12   concentration in the batch experiments. The slopes of the regression lines represent (α-1),

13   the isotopic fractionation for N and O.

14   **Figure 4.** Δδ^{15}N vs. Δδ^{18}O of nitrate for the batch experiments. The error bars show the

15   uncertainty in the isotope measurements.

16   **Figure. 5**. Nitrate concentrations by depth in the surroundings of the PRB. The different

17   depths of the multilevel wells are shown, as well as those of two conventional wells located

18   immediately upgradient (PZ10) and downgradient (PZ11) of the PRB (blue rectangle). The

19   well PZ4, located in the NW end of the PRB, is also shown. The size of the symbols is

20   proportional to the corresponding nitrate concentration value. Reference concentration

21   values are shown for comparison.

22   **Figure 6**. δ^{15}N$_{NO3}$ and δ^{18}O$_{NO3}$ in groundwater samples collected in March 2013 for the

23   multilevel wells and two conventional wells located immediately upgradient of the PRB (PZ4

24   and PZ10), as well as the isotope composition of the main potential nitrate sources:

25   fertilizers, soil nitrate and animal manure or sewage.

26   **Figure 7**. $\delta^{15}N_{NO3}$ vs. $\delta^{18}O_{NO3}$ in groundwater samples collected in March 2013 for the

27   multilevel wells and for two conventional wells located immediately upgradient of the PRB

28   (PZ4 and PZ10). The size of the bubbles is proportional to the nitrate concentration. The

29   denitrification models calculated with the Rayleigh equation using the isotopic fractionation

30   obtained in the PRB experiment and two different initial values, one affected by the lateral

31   input of PZ4 (% DEN Lateral) and one not affected (% DEN), are also shown.

32   **Table captions**

33   **Table 1.** Obtained N and O isotope fractionation values ($\varepsilon^{15}N$ and $\varepsilon^{18}O$) and isotope ratios

34   ($\varepsilon^{18}O/\varepsilon^{15}N$) for the laboratory experiments

Figure 1

Figure 2

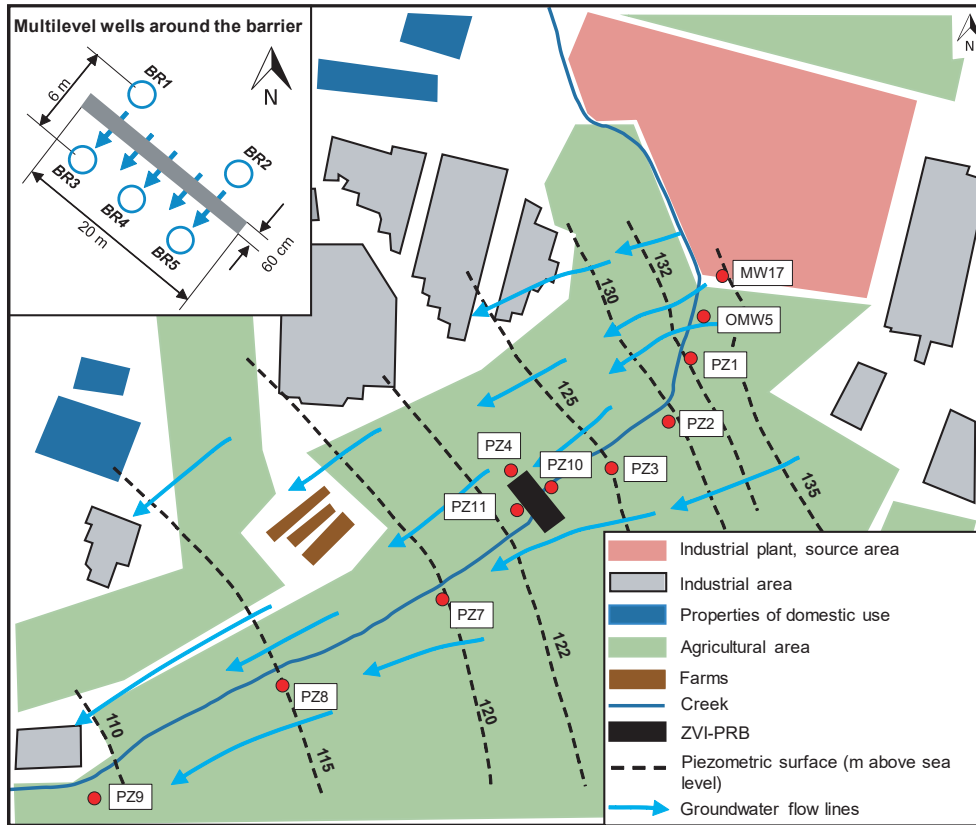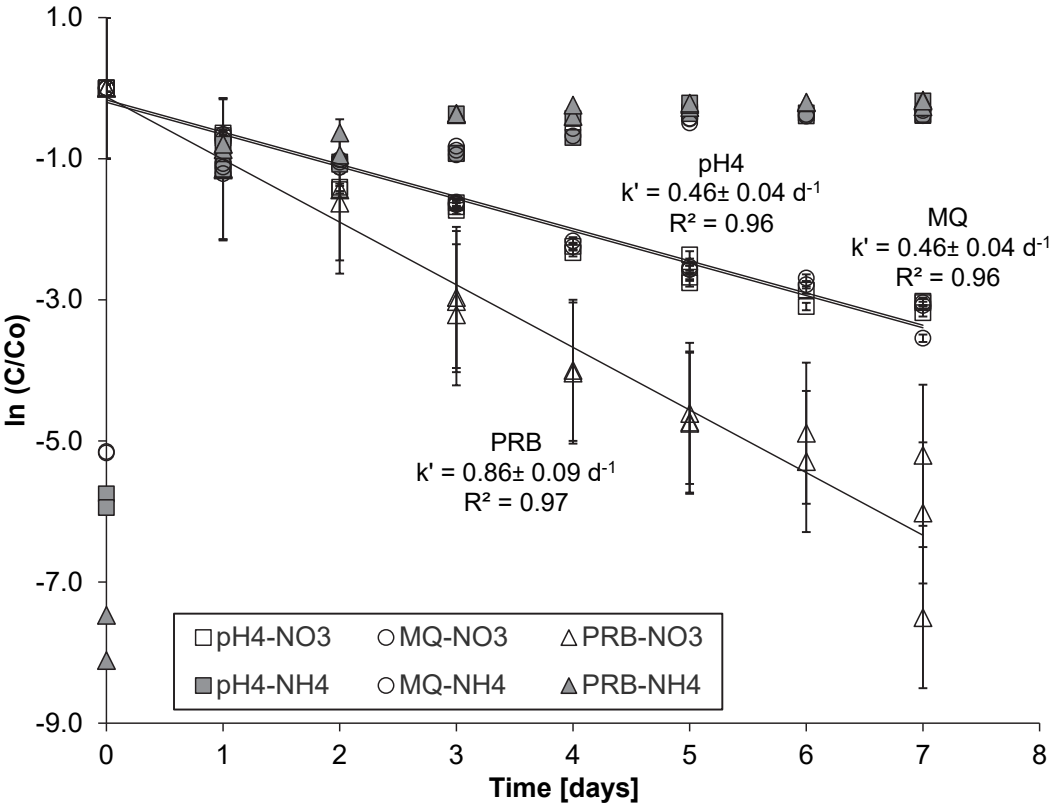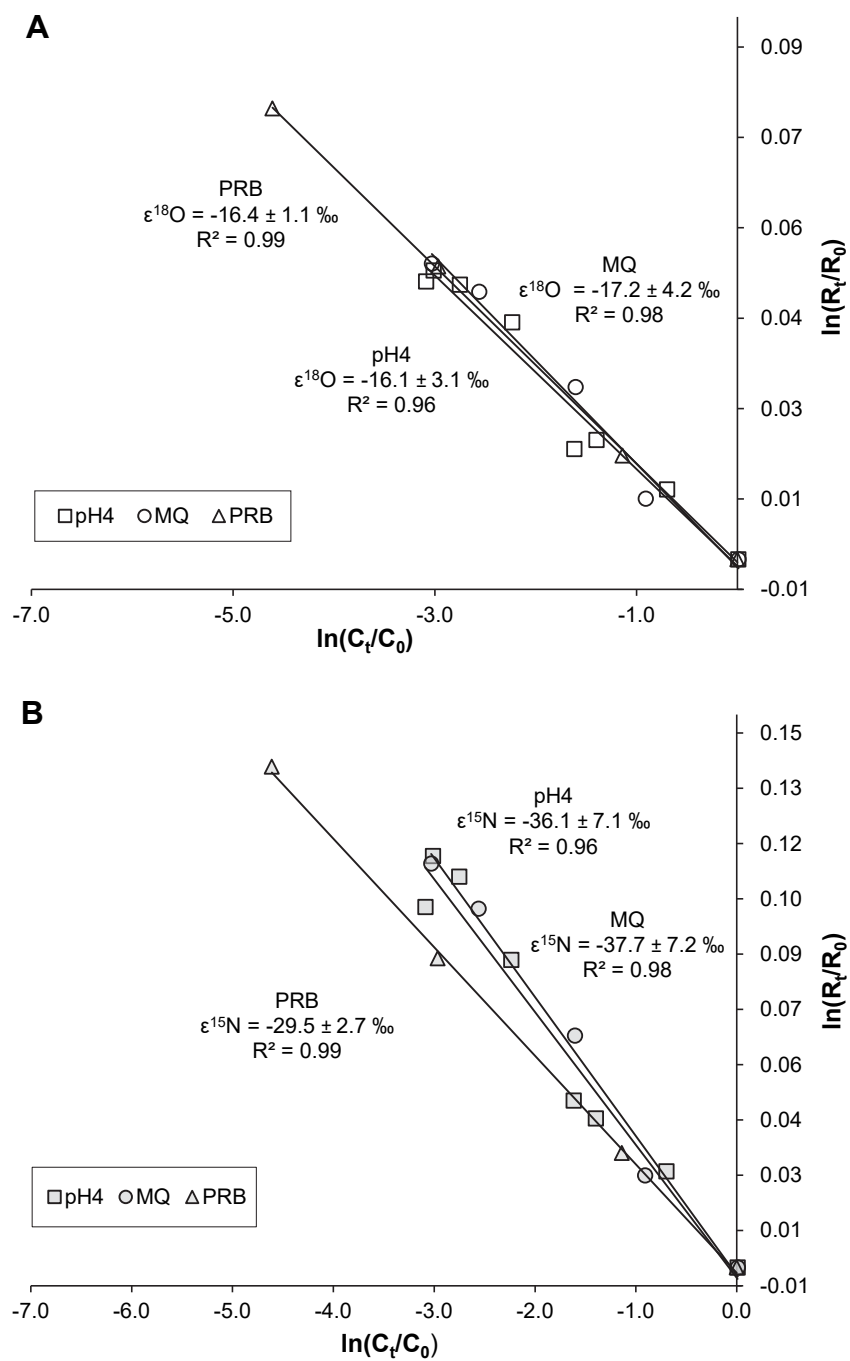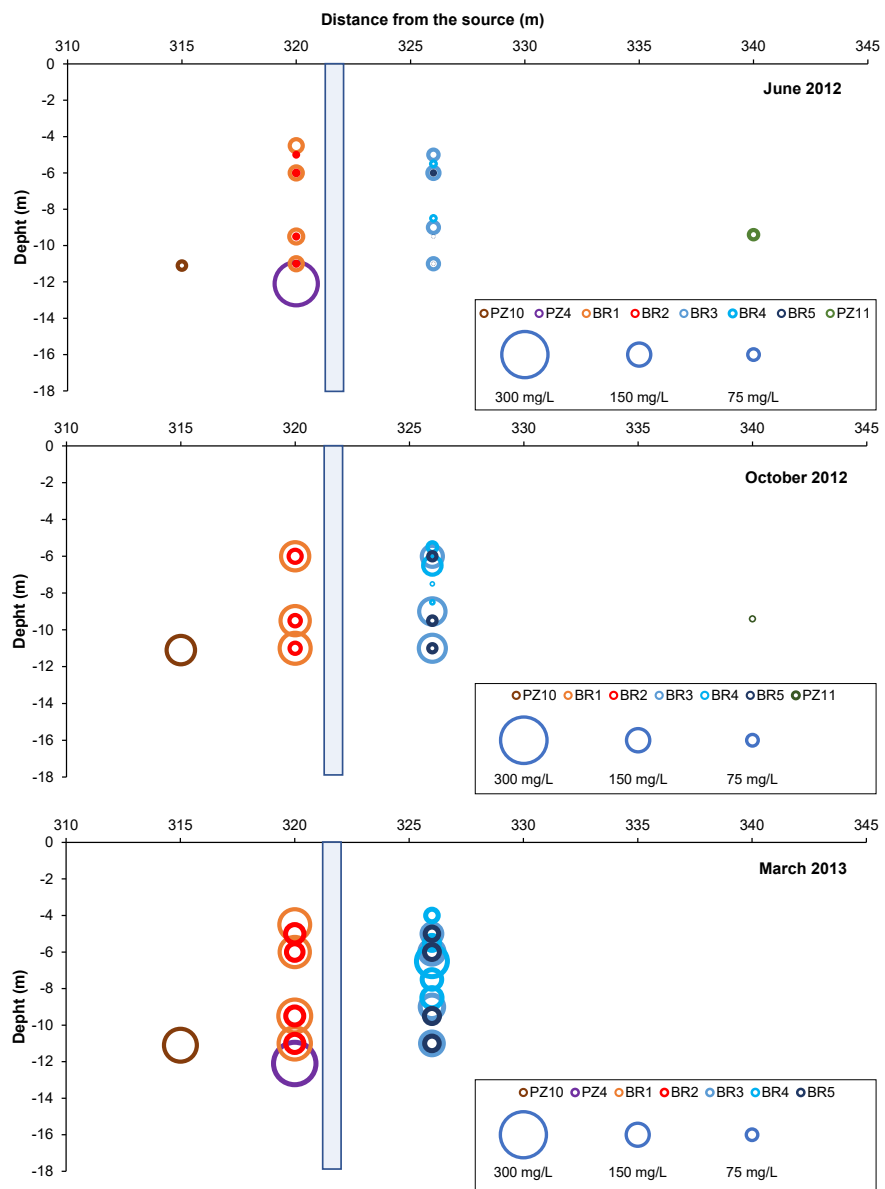# Figure 3

A

PRB
$\varepsilon^{18}O = -16.4 \pm 1.1$ ‰
$R^2 = 0.99$

MQ
$\varepsilon^{18}O = -17.2 \pm 4.2$ ‰
$R^2 = 0.98$

pH4
$\varepsilon^{18}O = -16.1 \pm 3.1$ ‰
$R^2 = 0.96$

□ pH4   ○ MQ   △ PRB

$\ln(R_t/R_0)$

$\ln(C_t/C_0)$

B

pH4
$\varepsilon^{15}N = -36.1 \pm 7.1$ ‰
$R^2 = 0.96$

MQ
$\varepsilon^{15}N = -37.7 \pm 7.2$ ‰
$R^2 = 0.98$

PRB
$\varepsilon^{15}N = -29.5 \pm 2.7$ ‰
$R^2 = 0.99$

□ pH4   ○ MQ   △ PRB

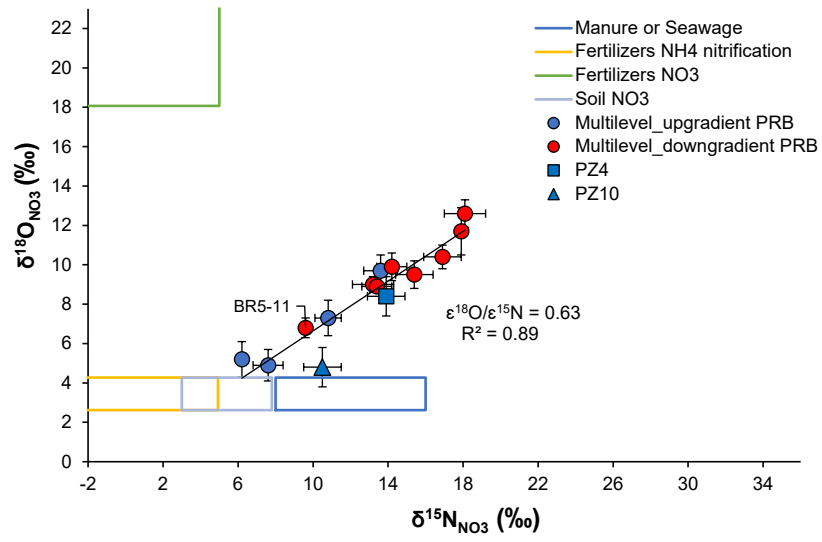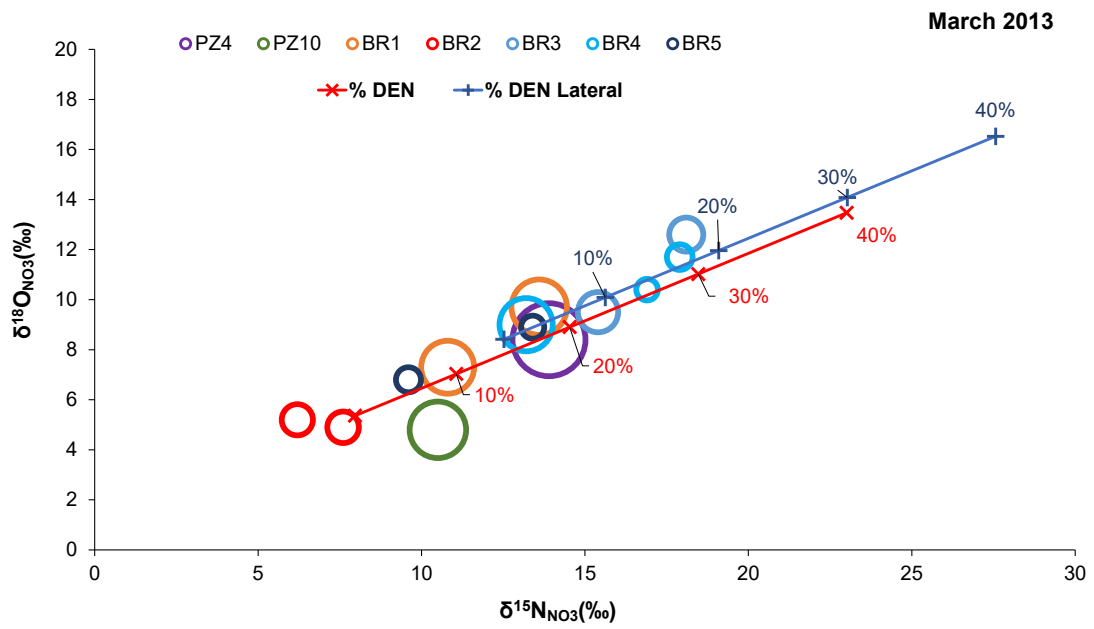$\ln(R_t/R_0)$

$\ln(C_t/C_0)$
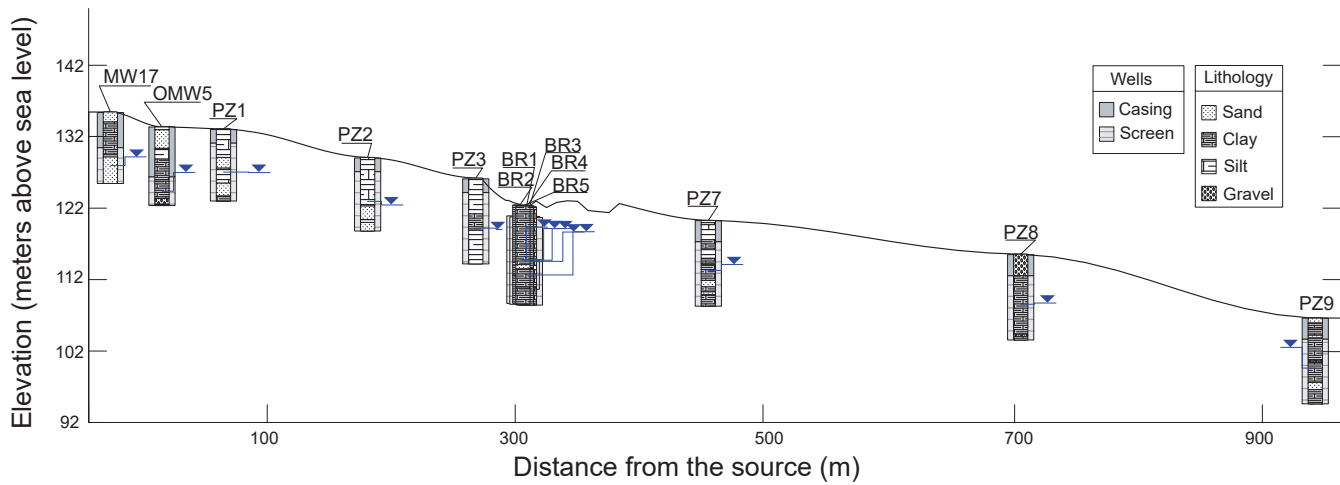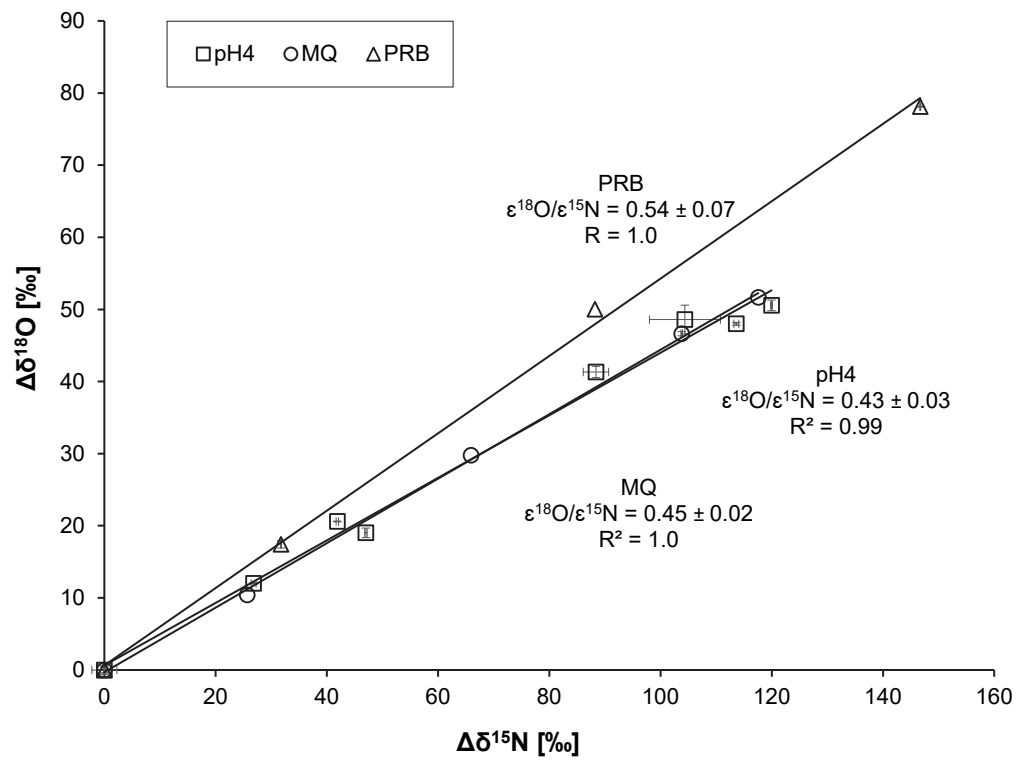
Figure 4

Figure 5

Figure 6

Figure 7

Table 1. Obtained N and O isotope fractionation values ($\varepsilon^{15}N$ and $\varepsilon^{18}O$) and isotope ratios ($\varepsilon^{18}O/\varepsilon^{15}N$) for the laboratory experiments

	$\varepsilon^{15}N \pm 95\%$ CI	$\varepsilon^{18}O \pm 95\%$ CI	$\varepsilon^{18}O/\varepsilon^{15}N \pm 95\%$ CI
pH4	-36.1 ± 7.1	-16.1 ± 3.1	0.43 ± 0.05
MQ	-37.7 ± 7.2	-17.2 ± 4.2	0.45 ± 0.02
combined pH4 & MQ	-36.6 ± 4.2	-16.4 ± 1.9	0.43 ± 0.02
PRB	-29.5 ± 2.7	-16.4 ± 1.0	0.54 ± 0.07
denitrification in the PRB experiment*	-20.5	-15.5	0.76

*Estimated using Eq. 9, assuming that in the PRB experiment two competing pathways occurred: ZVI-driven nitrate reduction (i.e. combined pH4 & MQ) and denitrification. See the text for detailed information